Detecting and Measuring Surface Area of Skin Lesions

Houman Mirzaalian-Dastjerdi[1,2], Dominique Töpfer[2], Michael Bangemann[3], Andreas Maier[1]

[1]Department of Computer Science 5, University of Erlangen-Nürnberg
[2]Softgate GmbH, Erlangen
[6]Praxisnetz Nürnberg Süd e.V.
houman.mirzaalian@fau.de

Abstract. The treatment of skin lesions of various kinds is a common task in clinical routine. Apart from wound care, the assessment of treatment efficacy plays an important role. Fully manual measurements and documentation of the healing process can be very cumbersome and imprecise. Existing technical solutions often require the user to delineate the lesion manually and rarely provide information on measurement precision or accuracy. We propose a method for segmenting and measuring lesions using a single image. Surface area of lesions on bent surfaces is estimated based on a paper ruler. Only roughly outlining the region of interest is required. Wound segmention evaluation was performed on 10 images, resulting in an accuracy of 0.98 ± 0.02. For surface measuring evaluation on 40 phantom images we found an absolute error of $0.32 \pm 0.27\,\mathrm{cm}^2$ and a relative error of $5.2 \pm 4.3\,\%$.

1 Introduction

Due to the prevalence of diseases such as diabetes, pressure ulcers etc., dealing with skin lesions is a common and frequent task in clinical routine. For monitoring treatment efficacy it is important to be able to measure the area of the skin lesion precisely. As pure manual methods (measuring width and height and approximating the shape by a rectangle or ellipse) are imprecise and cumbersome, a great deal of effort has gone into developing (semi-)automated techniques. In [1], a transparent grid film is placed on the lesion and its contour is marked manually. This allows for a more precise determination of the surface area, however, it is also time-consuming and due to direct contact of the film with the lesion, it may hurt the patient. Modern techniques such as laser scanners are requiring costly additional equipment [2]. That is why photographic techniques have gained more and more attention. In addition to already commercially available tools using manual delineation, there have been recent attempts to make use of 3D reconstructions from multiple images. The 3D model provides geometric information for measuring [3, 4]. The aim of this work is to investigate an easy, fast and low cost segmentation tool with high measurement accuracy. We propose a new method for both lesion segmentation and surface measurement based

on a single image taken with a commercial handheld digital camera or smartphone. From only one image, less information can be obtained than from a 3D model, especially in case of the wound being on a curved surface. For helping to estimate the local scale of the image even for curved surfaces, a flexible paper ruler is used.

2 Material and methods

Our approach comprises two main steps, wound segmentation and lesion surface area calculation. As only a single image is used, some conditions must be met during image acquisition for keeping the measurement error as low as possible. 1) The camera shall be perpendicular to the wound surface. 2) The wound shall be located in the center of the image (for minimizing lens distortion). 3) The ruler has to be placed parallel to the largest wound diameter as close as possible to it. Ideally, it should also reflect the curvature of the surface.

2.1 Wound segmentation

The user needs to provide a region of interest (ROI) including only wound and skin by drawing a contour (Fig. 1(a)). For classifying the pixels in the ROI into the classes skin and wound, a Random Forest (RF) classifier has been trained. Feature vectors were generated by applying a filter bank consisting of Gaussian, Difference of Gaussian, Sobel and Hessian filter using different values for the standard deviation.

The output of the RF is a probability map defining how likely it is that a single pixel belongs to wound or skin. Otsu's thresholding is applied to generate a binary mask. Finally, everything outside the ROI is discarded (Fig. 2).

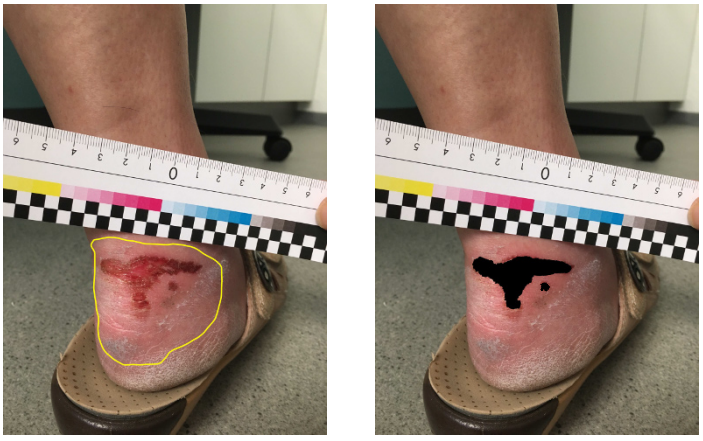

(a) (b)

Fig. 1. (a) Paper ruler and selected region of interest shown with yellow contour. (b) The ground truth image obtained using the modified Random Walker.

To facilitate creating the ground truth masks for training the RF, the Random Walker algorithm [5], with modified edge weight function based on Quaternion Color Curvature (QCC) [6] has been used (Fig. 1(b)).

2.2 Surface area measurement

For surface area calculation, the ruler should be first detected. As shown in (Fig. 3(a)), the ruler contains a checkboard pattern with known size for easy detection. The Structure Tensor filter is used for dividing the image into uniform regions, corners, and edges according to the tensor's eigenvalues [7] for each pixel. The high eigenvalues roughly correspond to the ruler skeleton shown in (Fig. 3(b)) and the low eigenvalues to corner points (Fig. 3(c)). Identification of checkboard points is based on comparing intensities in a region around the points. Fitting a curve to the local maxima of the distance transform of the points seperates them to upper and lower points (Fig. 3(d)). Moving along this curve allows finding pairs of corresponding points by detecting intensity changes across checkerboard edges. (Fig. 3(c)).

For obtaining the local measurement parameters, a heuristical approach is used: Consider two corresponding points (p_1, p_2) as shown in (Fig. 3(c)). Along the line defined by p_1 and p_2, points $p_3, p_4, \ldots$ are placed equidistantly using $d = \|p_1 - p_2\|_2$. Extrapolating each pair of points, a grid pattern covering the wound is obtained. For measuring, each quadrilateral in the grid is unwarped from perspective distortion [8] and mapped to a square. As the "true" size of the square is known from the definition of the ruler, measuring comes down to counting the wound pixels covered by the square and using the formula

$$A_w = \frac{N_w}{N} \cdot \text{area of square} \tag{1}$$

where N is the total number of pixels and N_w is the number of wound pixels in the square. Adding these results for all squares yields the surface area of the lesion.

Evaluation We recieved 50 images of skin lesions from clinical routine. They were not taken under controlled conditions and by different persons with different commercially available (smartphone) cameras. For training the RF, this

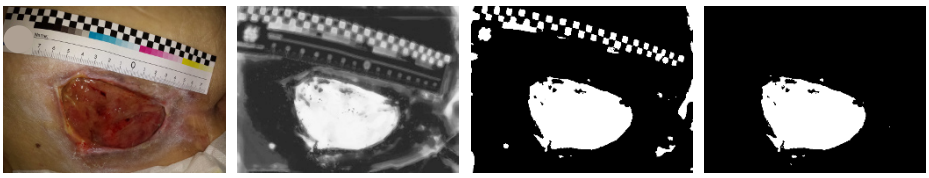

(a) (b) (c) (d)

Fig. 2. (a) Original image. (b) Probability map (result of Random Forest classifier). (c) Result of Otsu's filter. (d) Segmentation result after applying the ROI.

set of images was split into a training set of 40 images and a test set of 10 images. Splitting was done manually as the set contained multiple images for some patients. These images were all put in the training set.

As we do not know the true size of the lesions in the clinical images, evaluation of the measurements was performed using phantom images showing a geometric shape with known surface area (Fig. 3(a)). Forty phantom images with different geometric shapes of different sizes (ranging from 1.13–17.22 cm^2 were taken with an iPhone7's camera. For simulating practical use we also bent the shapes around cylindrical objects of different curvature and varied the angle of the camera slightly.

3 Results

For wound segmentation, we found a mean accuracy, sensitivity and specificity of 0.98 ± 0.02, 0.89 ± 0.13 and 0.99 ± 0.01, respectively, where accuracy is defined as the proportion of correctly classified pixels according to the ground truth. Fig. 4 shows a plot of these three values for each of the test images. Fig. 5 depicts three different results of segmented wounds.

For the measurement evaluation based on the phantom images we found an absolute error of $0.32 \pm 0.27\,\mathrm{cm}^2$ and a relative error of $5.2 \pm 4.3\,\%$. Tab. 1 shows the results grouped into flat images and images with lower and higher curvature.

Among these 40 images, 16 images consisted of eight pairs showing the same shape with slightly different size (differences ranging from 0.43 to 1.22 cm^2 and 7

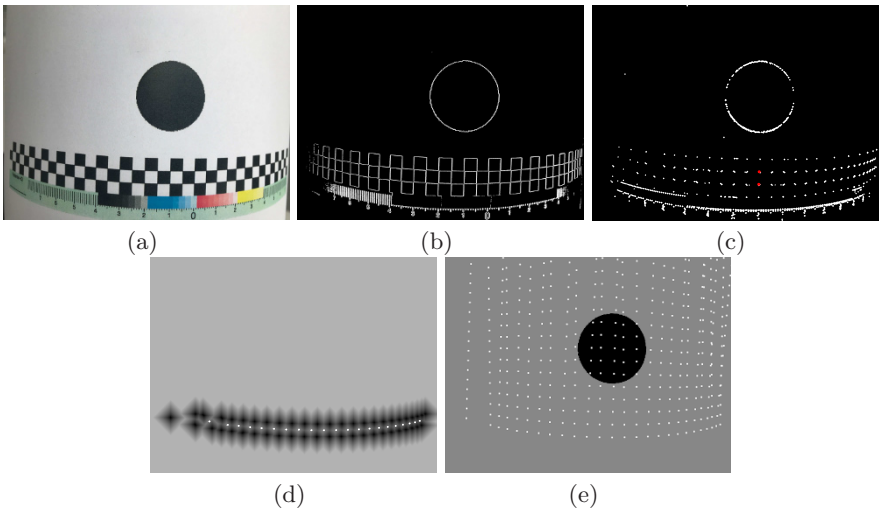

Fig. 3. (a) Phantom image. (b) Result of structure tensor filter containing high eigenvalues. (c) Result of structure tensor filter containing low eigenvalues. Two corresponding corner points p_1 and p_2 are highlighted (red). (d) Distance transform, local maxima shown with white points. (e) Obtained grid pattern and "wound segmentation" (black circle).

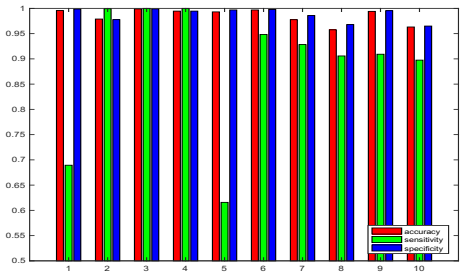

Fig. 4. The accuracy (red), sensitivity (green) and specificity (blue) parameters of wound segmentation of 10 patient wound images (bars were truncated for better visualization).

Table 1. Results for ruler-based measurements. Values for absolute and relative error are given as mean ± standard deviation.

Type of Image	absolute error (cm^2)	relative error (%)	Min Area (cm^2)	Max Area (cm^2)
Flat (N=20)	0.23±0.21	4.54±4.86	2.80	17.22
Low Curvature (N=12)	0.42±0.34	5.03±2.98	1.13	9.73
High Curvature (N=8)	0.39±0.23	7.28±3.63	2.80	8.98
All (N=40)	0.32±0.27	5.24±4.29	1.13	17.22

to 15 %). The true mean of surface areas in the group of smaller shapes was $\mu_s = 5.57\,cm^2$ compared to $\mu_l = 6.33\,cm^2$ for the group of larger shapes. Even though the measurements reflect this difference ($\bar{\mu}_s = 5.73\,cm^2$ and $\bar{\mu}_l = 6.52\,cm^2$), a paired, one-tailed t-test did not yield a significant difference.

3.1 Discussion and conclusion

We presented first results of our method for segmenting and measuring skin lesions from a single image with acceptable error also for lesions on a bent surface. A limitation of this study is the small number of data. For segmentation we only could test our method on 10 images and a proper cross-validation was not possible due to having multiple images of the same lesion. Skin lesions are greatly varying in appearance (color and texture), so the approach must be tested using

(a) (b) (c)

Fig. 5. (a) and (b) Examples of good segmentations. (c) A weak segmentation result (the red region is misclassified as wound).

more training and test images. Also color correction (which was not addressed in this article) may help stabilizing the results [4].

For measuring the area, our method is still lacking the possibility to reject images not taken perpendicular to the wound surface. If the angle is only slightly changed, the errors can quickly increase. It was beyond the scope of this study, addressing this problem more systematically. Also here the sample size was quite small, which also could explain the non-significant result for detecting changes in surface area. We have also studied a different approach for extrapolating the ruler points based on the cross ratio [9]; as we quickly found this approach to be less stable and to have greater error, we did not pursue it further. In [3], the announced measurement error is approximately 10% for available photographic techniques and the precision may vary with wound size. We found comparable results for our method, however, so far we have only addressed evaluation based on phantom images. Also, a systematic precision analysis was out of the scope of this work, due to the small amount of clinical images that contained the ruler.

Providing a method for rejecting images taken from great angles and tools for correcting failed segmentations could improve our approach. Further research with more data is necessary for validating this method.

References

1. Foltynski P, Ladyzynski P, Wojcicki JM. A new smartphone-based method for wound area measurement. Artific Organs. 2014;38(4):346–352.
2. Liu X, Kim W, Schmidt R, et al. Wound measurement by curvature maps: a feasibility study. Phys Measure. 2006;27(11):1107.
3. Treuillet S, Albouy B, Lucas Y. Three-dimensional assessment of skin wounds using a standard digital camera. IEEE Trans Med Imaging. 2009;28(5):752–762.
4. Wannous H, Lucas Y, Treuillet S. Enhanced assessment of the wound-healing process by accurate multiview tissue classification. IEEE Trans Med Imaging. 2011;30(2):315–326.
5. Grady L. Random walks for image segmentation. IEEE Trans Pattern Anal Machine Intell. 2006;28(11):1768–1783.
6. Shi L, Funt B, Hamarneh G. Quaternion color curvature. In: Color and Imaging Conference. vol. 2008. Society for Imaging Science and Technology; 2008. p. 338–341.
7. Baghaie A, Yu Z. Structure tensor based image interpolation method. AEU Int J Electronic Comm. 2015;69(2):515–522.
8. Jagannathan L, Jawahar C. Perspective correction methods for camera based document analysis. In: Proc. First Int. Workshop on Camera-based Document Analysis and Recognition; 2005. p. 148–154.
9. Lei G. Recognition of planar objects in 3-D space from single perspective views using cross ratio. IEEE Trans Robotic Automat. 1990;6(4):432–437.